2024 European Control Conference (ECC)
June 25-28, 2024. Stockholm, Sweden

Sensor Fault Diagnosis in Autonomous Ships*

Tahiyatul Asfihani[1], Fadia Lutfiani[1], Augie Widyotriatmo[2], and Agus Hasan[3]

Abstract— **Autonomous ships heavily depend on their sensor systems for safe and efficient operation. When these critical sensor systems are compromised by faults, the entire autonomous operation is put at risk. Detecting and accurately estimating the magnitude of such faults becomes imperative to ensure the reliability and safety of autonomous ships. In response to this challenge, this paper presents a robust methodology built upon adaptive Kalman filter with forgetting factor to estimate the magnitude of sensor faults. What sets our approach apart is the innovative perspective taken towards fault diagnosis. Instead of treating the fault as an additional state variable within the system, we directly estimate the fault magnitude based on the available measurements. Our approach is demonstrated through extensive simulations, showcasing the effectiveness and resilience of the proposed method. The results highlight its potential to significantly enhance the dependability of autonomous ships in the face of sensor faults, contributing to their continued success in a wide range of real-world applications.**

I. INTRODUCTION

The advancement of autonomous ship technology has been rapid, driven by the increasing demand for applications such as cargo delivery, defense operations, search and rescue missions, and even passenger transportation [1]. Autonomous ships are equipped with an array of sensors, including GNSS (Global Navigation Satellite System), LIDAR (Light Detection And Ranging), RADAR (Radio Detection And Ranging), Camera, and IMU (Inertial Measurement Unit), which provide vital data for determining their precise position and environmental conditions. This data is instrumental in designing the guidance and control systems necessary to fulfill the ship's intended tasks [2].

However, the reliability of these sensors can be compromised due to a variety of factors, such as material degradation, physical damage, or malicious attacks [3]. Sensor faults can lead to misinterpretations of actual conditions, potentially preventing the ship from achieving its objectives. In the worst-case scenario, these faults can result in the ship becoming lost or causing accidents [4]. For instance, consider a situation where a ship's GNSS sensor is tampered with or hacked. The ship may receive misleading position data, causing it to deviate from its intended course and potentially becoming disoriented or lost [5].

To mitigate the risks associated with sensor faults and ensure the safety of autonomous ships, the ability to detect and quantify these faults is crucial. However, directly measuring the magnitude of sensor faults is not feasible, making fault diagnosis a critical concern in autonomous ship systems [6]. Accurate diagnosis of sensor faults is the first step in enabling the system to compensate for these faults effectively, thereby safeguarding the ship's operation and ensuring that it can fulfill its tasks reliably and securely.

A. Related work

Fault diagnosis for autonomous ships has garnered significant attention within the research community in recent years [7]. This heightened interest is due to the recognition of the critical role that fault diagnosis plays in ensuring the safe and reliable operation of autonomous maritime systems. Faults, which can manifest in various forms, encompass actuators, sensors, and the structural components of these vessels [8]. Actuator faults can include issues with propulsion systems, steering mechanisms, and other components responsible for maneuvering the ship. Detecting and diagnosing such faults is crucial for maintaining control and navigational capabilities. Sensor faults, as previously discussed, are of paramount concern. These faults can lead to incorrect data inputs, affecting the ship's perception of its environment, and consequently, its decision-making processes. Addressing sensor faults is vital for accurate navigation and safe operation. While less common, structural faults in the vessel itself, such as hull damage, can also impact the ship's integrity and seaworthiness. Detecting structural faults is essential for preventing catastrophic failures and ensuring the safety of the ship and its crew [9].

The field of fault diagnosis has seen the development of a wide array of methods and techniques aimed at identifying and mitigating faults in complex systems. These methods have evolved to address the specific challenges and requirements of diverse applications. A comprehensive survey by Gao, et al. [10], provides an overview of various fault diagnosis techniques, including model-based methods, data-driven approaches, and hybrid strategies. It also discusses the challenges specific to sensor systems. Guo, et al. [11], introduced H-Infinity Kalman filtering as a robust approach for sensor fault diagnosis in autonomous ships. This methodology focuses on estimating sensor faults directly from measurements, enhancing fault detection and system resilience. The use of machine learning algorithms for sensor fault detection is explored in works like Cheliotis, et al. [12] and Diget, et al. [13]. These techniques leverage historical data to detect abnormal sensor behavior and contribute to autonomous system safety. Geng, et al. [14], investigated the role of sensor redundancy and data fusion techniques

*This work was supported by Equinor.

[1]Tahiyatul Asfihani and Fadia Lutfiani are affiliated with Department of Mathematics, Institut Teknologi Sepuluh Nopember, Indonesia.

[2]Augie Widyotriatmo is affiliated with Instrumentation and Control Research Group, Bandung Institute of Technology, Bandung 40132, Indonesia.

[3]Agus Hasan is affiliated with Department of ICT and Natural Sciences, Norwegian University of Science and Technology, Norway. Corresponding email: agus.hasan@ntnu.no.

Copyright ©2024 EUCA

in enhancing fault tolerance. Redundant sensors can provide backup information to validate sensor data and detect inconsistencies. In the area of robust fault diagnosis methods, several noteworthy contributions have been made by researchers. These methods offer innovative approaches to estimate both the system's state and faults simultaneously, ensuring the reliability and safety of complex systems. Ticlea, et al. introduced an approach that enables the estimation of both the system's state and system faults concurrently [15]. This method is based on a discrete deterministic formulation of an adaptive observer, which draws inspiration from the work presented by Besançon, et al. in [16]. The simulation results in the study by Ticlea, et al. demonstrate the convergence of their estimation method. Notably, one of the advantages of this approach is the flexibility to adjust the tuning parameter, denoted as λ. This parameter allows for the fine-tuning of the convergence rates for both state estimation and system fault estimation. This adaptability is valuable for customizing the method to specific system requirements and dynamics. Another significant contribution to simultaneous state and system fault estimation comes from Zhang [17]. His method is tailored for actuator fault diagnosis and is rooted in the Kalman Filter framework, designed for discrete linear stochastic systems. These methodologies aim to not only estimate the system's state accurately but also identify and quantify any potential faults within the system. This is essential for maintaining system performance and safety in applications where reliability is paramount.

Although significant progress has been made in the field of fault diagnosis for various systems, it is evident that sensor fault diagnosis has received relatively less attention. This is primarily attributed to the inherent complexities and challenges associated with addressing sensor faults. In many systems, especially in autonomous ships, a multitude of sensors are employed to capture diverse aspects of the environment and the system itself. Each sensor can potentially exhibit unique fault patterns, making it challenging to design a unified diagnosis framework. Furthermore, autonomous systems often incorporate redundancy in their sensor configurations to enhance reliability. However, dealing with sensor redundancy introduces complexities in fault diagnosis, as the system must discern between faulty and healthy sensors. Moreover, sensor measurements inherently exhibit random variations, which can sometimes mimic the effects of a fault. Distinguishing between natural measurement noise and actual sensor faults requires advanced statistical analysis. Despite these challenges, it is essential to recognize the significance of sensor fault diagnosis in ensuring the safety and reliability of autonomous systems. As the field continues to evolve, it is expected that more attention will be directed toward enhancing the robustness and dependability of sensor fault diagnosis in autonomous ships and other critical applications.

B. *Contribution of this paper*

This paper makes a significant contribution by introducing a novel sensor fault diagnosis algorithm tailored for autonomous ships. The primary focus of our approach is on the seamless integration of sensor measurements into the state space equations. We initiate this process by meticulously filtering the incoming data from the sensor systems and augmenting it within the framework of the state space equations. A crucial and distinguishing feature of our methodology is the subsequent application of an adaptive Kalman filter. What sets our approach apart is the innovative perspective taken towards fault diagnosis. Instead of treating the fault as an additional state variable within the system, we directly estimate the fault magnitude based on the available measurements. This deviation from the conventional approach to fault diagnosis significantly streamlines the process, resulting in a more efficient and accurate means of identifying and quantifying sensor faults. The presented algorithm has the potential to enhance the reliability and safety of autonomous ships by promptly and precisely diagnosing sensor issues, thereby ensuring uninterrupted and dependable operation in various real-world scenarios.

C. *Organization of this paper*

Section II of this paper is dedicated to problem formulation, where we establish the foundational context and set the stage for our research. Moving on to Section III, we delve into the core of our work by presenting the intricacies of our sensor fault diagnosis algorithm. This section provides a detailed exposition of the methodology, including the steps involved and the underlying principles that guide our approach. We discuss how we handle the filtering of sensor measurements, the augmentation of state space equations, and the application of the adaptive Kalman filter. In Section IV, we introduce the autonomous ship model, which serves as the basis for our research. Section V is devoted to numerical simulation. Here, we present the results of our simulations, providing empirical evidence of the effectiveness and robustness of our sensor fault diagnosis algorithm. Finally, in Section VI, we wrap up our findings and contributions, summarizing the key takeaways from our research.

II. PROBLEM FORMULATION

In this paper, we consider models of autonomous ships that can be transformed into the following form:

$$\boldsymbol{p}_k = \boldsymbol{A}_k\boldsymbol{p}_{k-1} + \boldsymbol{B}_k\boldsymbol{u}_k + \boldsymbol{w}_k \tag{1}$$

$$\boldsymbol{s}_k = \boldsymbol{C}_k\boldsymbol{p}_k + \boldsymbol{v}_k \tag{2}$$

Here, $\boldsymbol{p}_k \in \mathbb{R}^n$ represents the state of the autonomous ship at time step k, while $\boldsymbol{p}_{k-1}$ is the state at the previous time step. The terms $\boldsymbol{A}_k \in \mathbb{R}^{n\times n}$ and $\boldsymbol{B}_k \in \mathbb{R}^{n\times p}$ denote matrices that describe the dynamics and control inputs, respectively, and $\boldsymbol{u}_k \in \mathbb{R}^p$ is the control input at time k. Additionally, $\boldsymbol{w}_k \sim \mathcal{N}(\boldsymbol{0}, \boldsymbol{Q}_k) \in \mathbb{R}^n$ accounts for stochastic disturbances or uncertainties in the model. Furthermore, $\boldsymbol{s}_k \in \mathbb{R}^m$ represents the sensor measurements obtained from the autonomous ship at time step k. The matrix $\boldsymbol{C}_k \in \mathbb{R}^{m\times n}$ defines the relationship between the ship's state and the sensor measurements, and $\boldsymbol{v}_k \sim \mathcal{N}(\boldsymbol{0}, \boldsymbol{R}_k) \in \mathbb{R}^m$ represents sensor noise or measurement errors.

If we use the symbol $\boldsymbol{\theta} \in \mathbb{R}^m$ to represent the magnitude of sensor faults, the measurement equation (2) can be reformulated as follows:

$$\boldsymbol{s}_k = \boldsymbol{C}_k\boldsymbol{p}_k + \boldsymbol{\Psi}_k\boldsymbol{\theta} + \boldsymbol{v}_k \tag{3}$$

Here, $\boldsymbol{\Psi}_k \in \mathbb{R}^{m\times m}$ describes how sensor faults influence the measurements and is usually known. Equation (3) highlights the importance of considering sensor faults when interpreting sensor measurements in autonomous ships. The introduction of $\boldsymbol{\theta}$ and $\boldsymbol{\Psi}_k$ enables the model to capture the impact of sensor faults on the observed data, which is crucial for fault detection, diagnosis, and system reliability in the autonomous ships. By understanding and accounting for sensor faults, we can make more informed decisions and take appropriate corrective actions to ensure the accuracy and robustness of the autonomous ship's operation. In this paper, several key assumptions are made, including:

Assumption 1: The matrices $\boldsymbol{A}_k$, $\boldsymbol{B}_k$, $\boldsymbol{C}_k$, $\boldsymbol{\Psi}_k$, $\boldsymbol{Q}_k$, and $\boldsymbol{R}_k$ are upper bounded.

Assumption 2: The pair ($\boldsymbol{A}_k$, $\boldsymbol{C}_k$) is uniformly observable.

Assumption 3: The signals contained in the matrix $\boldsymbol{\Psi}_k$ are persistently exciting.

The primary goal of this research paper is to achieve a precise and reliable estimation of the magnitude represented by $\boldsymbol{\theta}$. In this context, $\boldsymbol{\theta}$ is a crucial parameter or variable of interest, which is typically associated with sensor faults or anomalies in the system.

III. SENSOR FAULT DIAGNOSIS ALGORITHM

The central concept explored in this paper is to apply a filtering process to the measurement signal $\boldsymbol{s}_k$, and this process is governed by the following equation:

$$\begin{aligned}\boldsymbol{z}_k &= (\boldsymbol{I} - \boldsymbol{A}_f\Delta t)\,\boldsymbol{z}_{k-1} + \boldsymbol{A}_f\Delta t\boldsymbol{C}_k\boldsymbol{p}_{k-1} \\ &\quad + \boldsymbol{A}_f\Delta t\boldsymbol{\Psi}_k\boldsymbol{\theta} + \boldsymbol{A}_f\Delta t\boldsymbol{v}_k \end{aligned}\tag{4}$$

Here, $\boldsymbol{z}_k \in \mathbb{R}^m$ is the filtered measurement signals, $\boldsymbol{A}_f \in \mathbb{R}^{m\times m}$ is a positive definite matrix, and $\Delta t \in \mathbb{R}$ is the filtered time step. Augmenting and rearranging (1) and (4), we have:

$$\boldsymbol{p}_k = \boldsymbol{A}_k\boldsymbol{p}_{k-1} + \boldsymbol{B}_k\boldsymbol{u}_k + \boldsymbol{w}_k \tag{5}$$

$$\begin{aligned}\boldsymbol{z}_k &= \boldsymbol{A}_f\Delta t\boldsymbol{C}_k\boldsymbol{p}_{k-1} + (\boldsymbol{I} - \boldsymbol{A}_f\Delta t)\,\boldsymbol{z}_{k-1} \\ &\quad + \boldsymbol{A}_f\Delta t\boldsymbol{\Psi}_k\boldsymbol{\theta} + \boldsymbol{A}_f\Delta t\boldsymbol{v}_k \end{aligned}\tag{6}$$

Let us denote

$$\boldsymbol{\xi}_k = \begin{pmatrix}\boldsymbol{p}_k \\ \boldsymbol{z}_k\end{pmatrix} \in \mathbb{R}^{n+m} \tag{7}$$

as the new augmented state. Then we have:

$$\boldsymbol{\xi}_k = \mathcal{A}_k\boldsymbol{\xi}_{k-1} + \mathcal{B}_k\boldsymbol{u}_k + \bar{\boldsymbol{\Psi}}_k\boldsymbol{\theta} + \bar{\boldsymbol{w}}_k \tag{8}$$

$$\mathcal{S}_k = \mathcal{C}_k\boldsymbol{\xi}_k \tag{9}$$

where

$$\mathcal{A}_k = \begin{pmatrix}\boldsymbol{A}_k & \boldsymbol{0} \\ \boldsymbol{A}_f\Delta t\boldsymbol{C}_k & \boldsymbol{I} - \boldsymbol{A}_f\Delta t\end{pmatrix} \in \mathbb{R}^{(n+m)\times(n+m)} \tag{10}$$

$$\mathcal{B}_k = \begin{pmatrix}\boldsymbol{B}_k \\ \boldsymbol{0}\end{pmatrix} \in \mathbb{R}^{(n+m)\times p} \tag{11}$$

$$\bar{\boldsymbol{\Psi}}_k = \begin{pmatrix}\boldsymbol{0} \\ \boldsymbol{A}_f\Delta t\boldsymbol{\Psi}_k\end{pmatrix} \in \mathbb{R}^{(n+m)\times m} \tag{12}$$

$$\bar{\boldsymbol{w}}_k = \begin{pmatrix}\boldsymbol{w}_k \\ \boldsymbol{A}_f\Delta t\boldsymbol{v}_k\end{pmatrix} \sim \mathcal{N}(\boldsymbol{0}, \bar{\boldsymbol{Q}}_k) \in \mathbb{R}^{(n+m)} \tag{13}$$

$$\mathcal{C}_k = \begin{pmatrix}\boldsymbol{0} & \boldsymbol{I}\end{pmatrix} \in \mathbb{R}^{m\times(n+m)} \tag{14}$$

In this paper, we have devised adaptive Kalman filter equations for the estimation of both sensor faults $\hat{\boldsymbol{\theta}}_k$ and the state $\hat{\boldsymbol{\xi}}_{k|k}$. The design of these equations is outlined below:

$$\hat{\boldsymbol{\theta}}_k = \hat{\boldsymbol{\theta}}_{k-1} + \boldsymbol{\Theta}_k\tilde{\mathcal{S}}_k \tag{15}$$

$$\begin{aligned}\hat{\boldsymbol{\xi}}_{k|k} &= \mathcal{A}_k\hat{\boldsymbol{\xi}}_{k-1|k-1} + \mathcal{B}_k\boldsymbol{u}_k + \bar{\boldsymbol{\Psi}}_k\hat{\boldsymbol{\theta}}_{k-1} + \boldsymbol{K}_k\tilde{\mathcal{S}}_k \\ &\quad + \boldsymbol{\Pi}_k\left[\hat{\boldsymbol{\theta}}_k - \hat{\boldsymbol{\theta}}_{k-1}\right]\end{aligned}\tag{16}$$

where the measurement error $\tilde{\mathcal{S}}_k$ is given by:

$$\tilde{\mathcal{S}}_k = \mathcal{S}_k - \mathcal{C}_k\left[\mathcal{A}_k\hat{\boldsymbol{\xi}}_{k-1|k-1} + \mathcal{B}_k\boldsymbol{u}_k + \bar{\boldsymbol{\Psi}}_k\hat{\boldsymbol{\theta}}_{k-1}\right] \tag{17}$$

The adaptive Kalman filter employs three distinct gains, specifically denoted as $\boldsymbol{K}_k \in \mathbb{R}^{(n+m)\times m}$, $\boldsymbol{\Pi}_k \in \mathbb{R}^{(n+m)\times m}$, and $\boldsymbol{\Theta}_k \in \mathbb{R}^{m\times m}$. The Kalman gain $\boldsymbol{K}_k$ is computed through the following process:

$$\boldsymbol{P}_{k|k-1} = \mathcal{A}_k\boldsymbol{P}_{k-1|k-1}\mathcal{A}_k^\intercal + \bar{\boldsymbol{Q}}_k \tag{18}$$

$$\boldsymbol{\Sigma}_k = \mathcal{C}_k\boldsymbol{P}_{k|k-1}\mathcal{C}_k^\intercal \tag{19}$$

$$\boldsymbol{K}_k = \boldsymbol{P}_{k|k-1}\mathcal{C}_k^\intercal\boldsymbol{\Sigma}_k^{-1} \tag{20}$$

$$\boldsymbol{P}_{k|k} = \left[\boldsymbol{I} - \boldsymbol{K}_k\mathcal{C}_k\right]\boldsymbol{P}_{k|k-1} \tag{21}$$

Here, $\boldsymbol{P}_{k|k} \in \mathbb{R}^{(n+m)\times(n+m)}$ is the covariance matrix of the state estimate and $\boldsymbol{\Sigma}_k \in \mathbb{R}^{m\times m}$ is the innovation covariance matrix. The noise covariance matrix $\bar{\boldsymbol{Q}}_k \in \mathbb{R}^{(n+m)\times(n+m)}$ is computed using the following formula [18]:

$$\bar{\boldsymbol{Q}}_k = a\bar{\boldsymbol{Q}}_{k-1} + (1-a)\left(\boldsymbol{K}_k\tilde{\mathcal{S}}_k\tilde{\mathcal{S}}_k^\intercal\boldsymbol{K}_k^\intercal\right) \tag{22}$$

where a is the tuning parameter. The observer gains $\boldsymbol{\Pi}_k$ and $\boldsymbol{\Theta}_k$ are obtained from [17]:

$$\boldsymbol{\Pi}_k = \left[\boldsymbol{I} - \boldsymbol{K}_k\mathcal{C}_k\right]\mathcal{A}_k\boldsymbol{\Pi}_{k-1} + \left[\boldsymbol{I} - \boldsymbol{K}_k\mathcal{C}_k\right]\bar{\boldsymbol{\Psi}}_k \tag{23}$$

$$\boldsymbol{\Omega}_k = \mathcal{C}_k\mathcal{A}_k\boldsymbol{\Pi}_{k-1} + \mathcal{C}_k\bar{\boldsymbol{\Psi}}_k \tag{24}$$

$$\boldsymbol{\Lambda}_k = \left[\lambda\boldsymbol{\Sigma}_k + \boldsymbol{\Omega}_k\boldsymbol{S}_{k-1}\boldsymbol{\Omega}_k^\intercal\right]^{-1} \tag{25}$$

$$\boldsymbol{\Theta}_k = \boldsymbol{S}_{k-1}\boldsymbol{\Omega}_k^\intercal\boldsymbol{\Lambda}_k \tag{26}$$

$$\boldsymbol{S}_k = \frac{1}{\lambda}\boldsymbol{S}_{k-1} - \frac{1}{\lambda}\boldsymbol{S}_{k-1}\boldsymbol{\Omega}_k^\intercal\boldsymbol{\Lambda}_k\boldsymbol{\Omega}_k\boldsymbol{S}_{k-1} \tag{27}$$

where the auxiliary variables $\boldsymbol{\Omega}_k \in \mathbb{R}^{m\times m}$, $\boldsymbol{\Lambda}_k \in \mathbb{R}^{m\times m}$, and $\boldsymbol{S}_k \in \mathbb{R}^{m\times m}$.

Theorem 1: The mathematical expectations $\mathbb{E}\tilde{\boldsymbol{\xi}}_{k|k}$ and $\mathbb{E}\tilde{\boldsymbol{\theta}}_k$ tend to zero exponentially when $k \to \infty$.

Proof: The theorem's proof relies on the foundation established in [17]. In the context of this paper, our objective is to demonstrate that Assumptions 1 through 3 hold true for equations (8) to (9). The boundedness of equations (10) to (14) is evident under the conditions set forth in Assumptions 1. Assumptions 2, on the other hand, are contingent upon the condition that $\boldsymbol{I} \neq \boldsymbol{A}_f \Delta t$. Finally, Assumption 3 is fulfilled when the signals encompassed within the matrix $\boldsymbol{\Psi}_k$ exhibit persistent excitation. ■

IV. THE SHIP MODEL

In the literature, a diverse range of models for autonomous ships exists, spanning from the simplest and most rudimentary representations to highly intricate and sophisticated ones. The selection of a particular model hinges on the specific application's requirements and the desired level of fidelity. Notably, in this paper, the focus centers on sensor fault diagnosis, and the methodology is crafted around a widely accepted and shared model for ships. The dynamics of the ship are represented by the following set of equations:

$$\dot{x}(t) = U(t)\cos(\chi(t)) \tag{28}$$
$$\dot{y}(t) = U(t)\sin(\chi(t)) \tag{29}$$
$$\dot{U}(t) = a(t) \tag{30}$$
$$\dot{\chi}(t) = r(t) \tag{31}$$

In this model, $x(t)$ and $y(t)$ correspond to the ship's positions in the horizontal plane, $U(t)$ represents its velocity, and $\chi(t)$ denotes the course angle. The control inputs for the model are the acceleration $a(t)$ and the course rate $r(t)$. These model encapsulates the ship's kinematic behavior, providing a foundation for understanding its motion in terms of position, velocity, and control inputs.

Upon discretizing the model using Euler's method and adding the noise into the model, we obtain:

$$x_k = x_{k-1} + \Delta t U_{k-1}\cos(\chi_{k-1}) + w_k^1 \tag{32}$$
$$y_k = y_{k-1} + \Delta t U_{k-1}\sin(\chi_{k-1}) + w_k^2 \tag{33}$$
$$U_k = U_{k-1} + \Delta t a_k + w_k^3 \tag{34}$$
$$\chi_k = \chi_{k-1} + \Delta t r_k + w_k^4 \tag{35}$$

The nonlinear terms present in equations (32) and (33) can be approximated and linearized through the application of Taylor series expansion. In our paper, the application of linearization will be specifically denoted as the adaptive extended Kalman filter [19]. In practical implementations, it is crucial to replace the matrix $\mathcal{A}_k$ in (18), (23), and (24) with the Jacobian matrix to ensure accurate linear approximations of the system dynamics. For the sake of clarity and without sacrificing generality, we shall consider a specific example where $\boldsymbol{A}_f$ is set to a value of $5\boldsymbol{I}$ and $\boldsymbol{\Psi}_k = \boldsymbol{I}$. This choice is made to illustrate the methodology effectively. The filtered sensor measurement are given by:

$$z_k^1 = (1-5\Delta t)z_{k-1}^1 + 5\Delta t x_{k-1} + 5\Delta t\theta^1 + 5v_k^1 \tag{36}$$
$$z_k^2 = (1-5\Delta t)z_{k-1}^2 + 5\Delta t y_{k-1} + 5\Delta t\theta^2 + 5v_k^2 \tag{37}$$
$$z_k^3 = (1-5\Delta t)z_{k-1}^3 + 5\Delta t U_{k-1} + 5\Delta t\theta^3 + 5v_k^3 \tag{38}$$
$$z_k^4 = (1-5\Delta t)z_{k-1}^3 + 5\Delta t \chi_{k-1} + 5\Delta t\theta^4 + 5v_k^4 \tag{39}$$

The filtered sensor measurement is given as the following vector:

$$\boldsymbol{z}_k = \begin{pmatrix} z_k^1 \\ z_k^2 \\ z_k^3 \\ z_k^4 \end{pmatrix} \tag{40}$$

Based on the derived expression, it is crucial to select a time step that is not equal to 0.2 seconds, as the specified time step would lead to the violation of Assumption 2. By augmenting the system's nonlinear equations represented in (32) through (35) with the provided equations, we obtain the final state space equations (8) and (9) with:

$$\mathcal{A}_k = \begin{pmatrix} \boldsymbol{I} & \boldsymbol{0} \\ 5\boldsymbol{I}\Delta t & \boldsymbol{I} - 5\boldsymbol{I}\Delta t \end{pmatrix} \tag{41}$$
$$\mathcal{B}_k = \begin{pmatrix} \boldsymbol{B}_k \\ \boldsymbol{0} \end{pmatrix} \tag{42}$$
$$\bar{\boldsymbol{\Psi}}_k = \begin{pmatrix} \boldsymbol{0} \\ 5\boldsymbol{I}\Delta t \end{pmatrix} \tag{43}$$
$$\bar{\boldsymbol{w}}_k = \begin{pmatrix} \boldsymbol{w}_k \\ 5\boldsymbol{I}\Delta t \boldsymbol{v}_k \end{pmatrix} \tag{44}$$
$$\mathcal{C}_k = \begin{pmatrix} \boldsymbol{0} & \boldsymbol{I} \end{pmatrix} \tag{45}$$

where $\boldsymbol{I}$ is an identity matrix with appropriate dimension. The objective is to estimate the sensor fault parameter:

$$\boldsymbol{\theta} = \begin{pmatrix} \theta^1 \\ \theta^2 \\ \theta^3 \\ \theta^4 \end{pmatrix} \tag{46}$$

For this system, the Jacobian matrix is given by:

$$\boldsymbol{F}_k = \begin{pmatrix} 1 & 0 & \Delta t\cos(\hat{\chi}_{k-1}) & -\Delta t\hat{U}_{k-1}\sin(\hat{\chi}_{k-1}) & 0 & 0 & 0 & 0 \\ 0 & 1 & \Delta t\sin(\hat{\chi}_{k-1}) & \Delta t\hat{U}_{k-1}\cos(\hat{\chi}_{k-1}) & 0 & 0 & 0 & 0 \\ 0 & 0 & 1 & 0 & 0 & 0 & 0 & 0 \\ 0 & 0 & 0 & 1 & 0 & 0 & 0 & 0 \\ 5\Delta t & 0 & 0 & 0 & 1-5\Delta t & 0 & 0 & 0 \\ 0 & 5\Delta t & 0 & 0 & 0 & 1-5\Delta t & 0 & 0 \\ 0 & 0 & 5\Delta t & 0 & 0 & 0 & 1-5\Delta t & 0 \\ 0 & 0 & 0 & 5\Delta t & 0 & 0 & 0 & 1-5\Delta t \end{pmatrix} \tag{47}$$

V. NUMERICAL SIMULATIONS

We have now reached a pivotal stage to subject our proposed methodology to rigorous testing through numerical simulations. This crucial phase enables us to assess the robustness, versatility, and adaptability of our approach under different scenarios and conditions, thereby contributing to a more comprehensive understanding of its capabilities and limitations.

A. Fault Detection and Estimation

The initial simulation spans a duration of 40 seconds, with a time step Δt set at 0.01 seconds. The system is subjected to inputs represented by the acceleration and course rate, which are essential control parameters governing the ship's behavior and navigation. This simulation serves as an initial test case to evaluate the system's response under these specified conditions and forms a foundational aspect of our analysis, offering insights into the system's performance and behavior over the given time frame. Faults are intentionally introduced into the system at two distinct time points, namely at $t = 10$ seconds and $t = 20$ seconds, and these faults affect all sensors responsible for measuring the state variables x, y, U, and χ. Initial parameters for the simulation include: $\boldsymbol{P}_{0|0} = \boldsymbol{I}$, $\bar{\boldsymbol{Q}}_0 = 0.001\boldsymbol{I}$, $a = 0.999$, $\boldsymbol{\Pi}_0 = \boldsymbol{0}$, and $\boldsymbol{S}_0 = \boldsymbol{I}$.

Figure 1 provides a visual representation of the autonomous ship's position in the horizontal plane. It is evident from the plot that the proposed method for sensor fault diagnosis demonstrates remarkable accuracy in estimating the ship's position. This capability is pivotal for ensuring precise navigation and control. Additionally, Figure 2 extends the assessment by showcasing the method's effectiveness in estimating both the velocity and the course angle of the ship. The plotted results highlight the method's capacity to accurately infer these critical dynamic parameters. These observations underscore the method's proficiency in providing comprehensive state estimation for the autonomous ship, a fundamental aspect of autonomous navigation and control that is vital for various maritime applications.

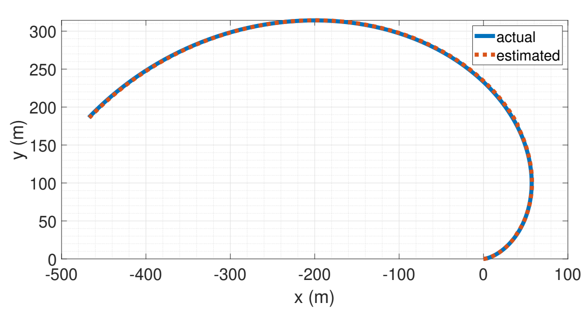

Fig. 1. Position of the autonomous ship started at (0,0).

The estimated sensor faults are presented in both Figure 3 and Figure 4, providing a comprehensive view of the fault diagnosis process. Notably, in Figure 4, the estimation procedure successfully converges to the actual fault values. This convergence is an encouraging outcome, indicating the method's proficiency in accurately identifying and tracking sensor faults over time.

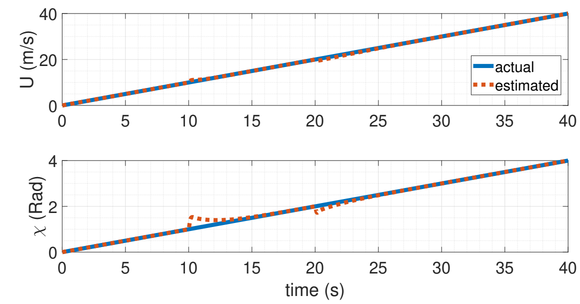

Fig. 2. Ship velocity with acceleration = $1m/s^2$ (top) and ship course angle with course rate $0.1Rad/s^2$ (bottom).

Conversely, Figure 3 reveals a distinct behavior in the fault estimation process. Here, the estimation does not exhibit convergence to the actual fault values. The underlying reason for this divergence can be attributed to a specific aspect of the fault model. More precisely, it is observed that only the fault parameters θ^3 and θ^4 remain persistently exciting due to their interaction with the input variables U and χ. In contrast, θ^1 and θ^2 lack this persistent excitation, which hinders their accurate estimation. This observation underscores the importance of ensuring that all fault parameters remain consistently excited for effective and reliable sensor fault diagnosis.

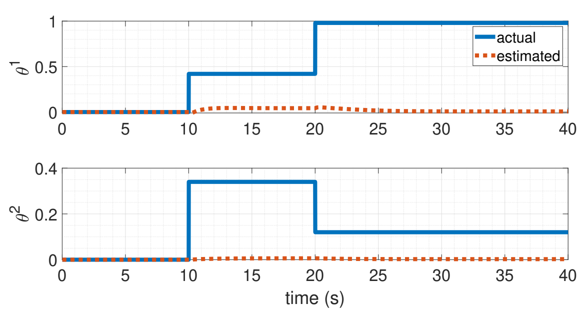

Fig. 3. Estimation of sensor faults pertains specifically to the position sensors x and y.

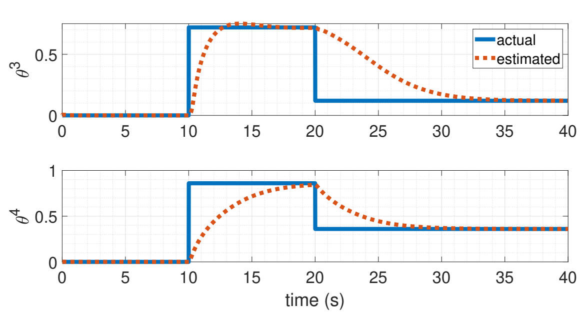

Fig. 4. Estimation of sensor faults pertains specifically to the velocity sensor U and course angle sensor χ.

B. Parameter Sensitivity Analysis

We conducted a sensitivity analysis to assess the impact of parameters that govern the convergence rate of the estimation process. These key parameters include the filtering measurement matrix $\boldsymbol{A}_f$ and the forgetting factor λ. Figure 5 presents a series of plots showcasing the estimation behavior under various values of λ. Notably, it is evident that as λ is increased, the convergence rate of the estimation process becomes slower. In Figure 6, the analysis explores the influence of varying $\boldsymbol{A}_f$ values on the convergence rate. It is observed that increasing $\boldsymbol{A}_f$ accelerates the convergence rate; however, this change also introduces overshooting in the estimation process. These findings underscore the delicate balance required when fine-tuning parameters in sensor fault diagnosis algorithms, as adjustments to λ and $\boldsymbol{A}_f$ can have significant implications on the estimation performance and stability.

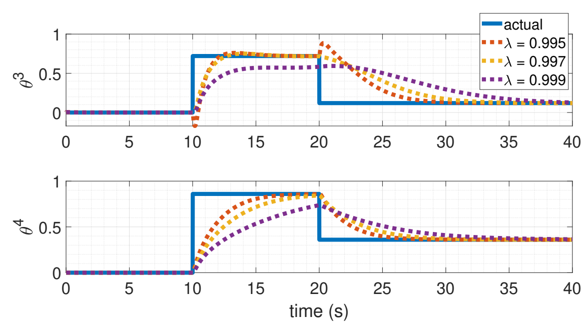

Fig. 5. Estimation of the fault parameters with $\boldsymbol{A}_f = 5\boldsymbol{I}$ with different λ.

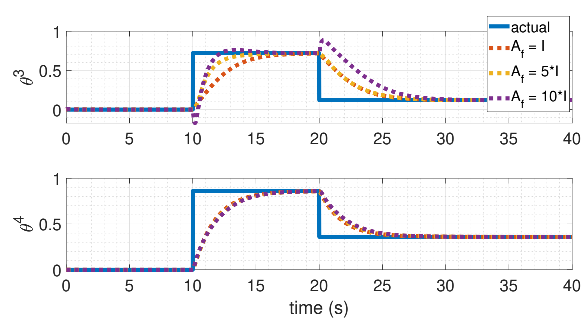

Fig. 6. Estimation of the fault parameters with $\lambda = 0.995$ with different $\boldsymbol{A}_f$.

VI. CONCLUSIONS

In this paper, we introduced a novel sensor fault diagnosis algorithm built upon the principles of the adaptive Kalman filter. A notable feature of our approach is its adaptability to nonlinear systems, making it well-suited for a wide range of maritime applications. By employing this methodology, we not only estimate the system's state accurately but also concurrently assess fault parameters, ensuring a comprehensive understanding of the system's health. Our extensive simulations, varying parameters across different scenarios, have consistently demonstrated the robustness and reliability of our method. A noteworthy limitation of the proposed method is its ability to accurately estimate parameter faults. Specifically, the method excels in accurate estimation only when the state linked to the sensor fault exhibits persistent excitation. This requirement poses a constraint on the method's effectiveness, as it implies that in scenarios where the state associated with the sensor fault lacks consistent excitation, the accuracy and reliability of parameter fault estimation may be compromised.

REFERENCES

[1] Z. Liu, Y. Zhang, X. Yu, and C. Yuan, "Unmanned surface vehicles: An overview of developments and challenges," *Annual Reviews in Control*, vol. 41, pp. 71–93, 2016.

[2] C. Edwards and C. P. Tan, "Sensor fault tolerant control using sliding mode observers," *Control Engineering Practice*, vol. 14, no. 8, pp. 897–908, 2006.

[3] A. Hasan, A. Widyotriatmo, E. Fagerhaug, and O. Osen, "Predictive digital twins for autonomous ships," in *2023 IEEE Conference on Control Technology and Applications (CCTA)*. IEEE, 2023, pp. 1128–1133.

[4] A. Hasan, T. Asfihani, O. Osen, and R. T. Bye, "Leveraging digital twins for fault diagnosis in autonomous ships," *Ocean Engineering*, vol. 292, p. 116546, 2024.

[5] Y.-C. Liu, G. Bianchin, and F. Pasqualetti, "Secure trajectory planning against undetectable spoofing attacks," *Automatica*, vol. 112, p. 108655, 2020.

[6] K. Geng and S. Liu, "Robust path tracking control for autonomous vehicle based on a novel fault tolerant adaptive model predictive control algorithm," *Applied Sciences*, vol. 10, no. 18, p. 6249, 2020.

[7] R. Bhagavathi, D. K. M. Kufoalor, and A. Hasan, "Digital twin-driven fault diagnosis for autonomous surface vehicles," *IEEE Access*, vol. 11, pp. 41 096–41 104, 2023.

[8] A. Hasan, M. Tahavori, and H. S. Midtiby, "Model-based fault diagnosis algorithms for robotic systems," *IEEE Access*, vol. 11, pp. 2250–2258, 2023.

[9] A. Hasan and T. A. Johansen, "Model-based actuator fault diagnosis in multirotor uavs," in *2018 International Conference on Unmanned Aircraft Systems (ICUAS)*, 2018, pp. 1017–1024.

[10] Z. Gao, C. Cecati, and S. X. Ding, "A survey of fault diagnosis and fault-tolerant techniques—part i: Fault diagnosis with model-based and signal-based approaches," *IEEE Transactions on Industrial Electronics*, vol. 62, no. 6, pp. 3757–3767, 2015.

[11] M. Guo, C. Guo, and C. Zhang, "A framework of cubature-h/h-infinity -fault detection and robust h-infinity kalman filter of ship sins/gnss integrated system," *IEEE Access*, vol. 8, pp. 196 963–196 974, 2020.

[12] M. Cheliotis, I. Lazakis, and G. Theotokatos, "Machine learning and data-driven fault detection for ship systems operations," *Ocean Engineering*, vol. 216, p. 107968, 2020.

[13] E. L. Diget, A. Hasan, and P. Manoonpong, "Machine learning with echo state networks for automated fault diagnosis in small unmanned aircraft systems," in *2022 International Conference on Unmanned Aircraft Systems (ICUAS)*, 2022, pp. 1066–1072.

[14] W. Geng, D. Fu, and M. Wu, "Fault diagnosis and can bus/ethernet redundancy design of a monitoring and control system," in *Proceedings of the 9th International Conference on Computer Engineering and Networks*, 2021, pp. 1063–1070.

[15] A. Ţiclea and G. Besançon, "Adaptive observer design for discrete time ltv systems," *International journal of Control*, vol. 89, no. 12, pp. 2385–2395, 2016.

[16] G. Besancon, J. de León-Morales, and O. Huerta-Guevara, "On adaptive observers for state affine systems," *International journal of Control*, vol. 79, no. 06, pp. 581–591, 2006.

[17] Q. Zhang, "Adaptive kalman filter for actuator fault diagnosis," *Automatica*, vol. 93, pp. 333–342, 2018.

[18] S. Akhlaghi, N. Zhou, and Z. Huang, "Adaptive adjustment of noise covariance in kalman filter for dynamic state estimation," in *2017 IEEE power & energy society general meeting*. IEEE, 2017, pp. 1–5.

[19] M. Skriver, J. Helck, and A. Hasan, "Adaptive extended kalman filter for actuator fault diagnosis," in *2019 4th International Conference on System Reliability and Safety (ICSRS)*, 2019, pp. 339–344.